



Lab 1: Gamma Cross Sections

Diego Garza

October 14, 2021

1 Setup/Overview

This experiment was to measure the total interaction cross section for different gamma rays ranging from 31 keV to 1.27 MeV of a given absorber material. To do this, we must measure the fractional absorption of gamma rays from a particular energy source and plot the amount that passes through as an exponential decay, which is related via the decay constant. The decay constant of the exponential decay is related to the cross section by the equations 1 and 2.

$$\lambda = N \cdot \sigma \quad (1)$$

$$N = \rho Z/A \quad (2)$$

The experiment for gamma energy cross sections was set up with the source at the bottom decaying and releasing gamma rays. The absorber would absorb some of the electrons given off from gamma rays. The NaI crystal would scintillate to detect the electrons that did pass through. Then the photomultiplier tube would amplify the signal to generate more pulses of energy. These pulses are the counts that were measured by the software, UCS-30.

For this experiment, we used different combinations of different lead absorbers: a thin circular plate, a medium square plate, and a large, thick square plate.

2 Data

2.1 Spectra

After the photomultiplier tube would generate more electrons, the anode would detect the relevant electrons. The software would place the amount of electrons into histograms with bins of energy, or the software uses a "channel". The counts of each spectrum all had interesting features. Figures 1, 2, 3 all show clearly identified features from these spectra.

Many interesting features can be seen in all three spectra. Here there are plenty of overlaps of Compton shelves within the same source for different energy peaks. For example, the Na-22 spectra in figure 1 shows that the energy peak for 1.27 MeV seems to have its Compton Shelf bleed into the first 511 keV energy peak. This can be seen from what looks like two different backscatter peaks to the left of the 511 keV energy peak. Apart from Na-22's both energy peaks as well as Cs-137's 662 keV energy peak, the Compton edge is a bit harder to distinguish in all other energy peaks. The first 32 keV energy peak for Cs-137 is so close to the channel minimum that it is hard to distinguish between data to the left of the peak. The Barium spectra has so many overlapping effects that it is hard to distinguish a clearly defined Compton edge.

From the decay schemes on the wiki for the course, the overlapping effects for Barium are better understood, as can be seen in figure 4. There are many possible ways for Br-133 to decay to the stable Cs-133, so we can expect similar full energy peaks in the same range. Specifically, there are high

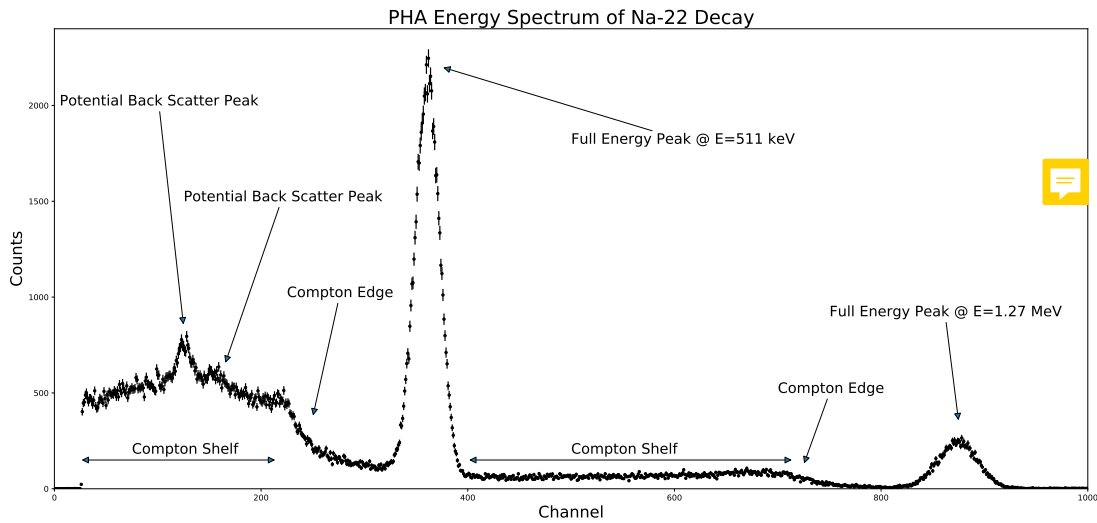


Figure 1: Full energy spectrum for Na-22 Decay

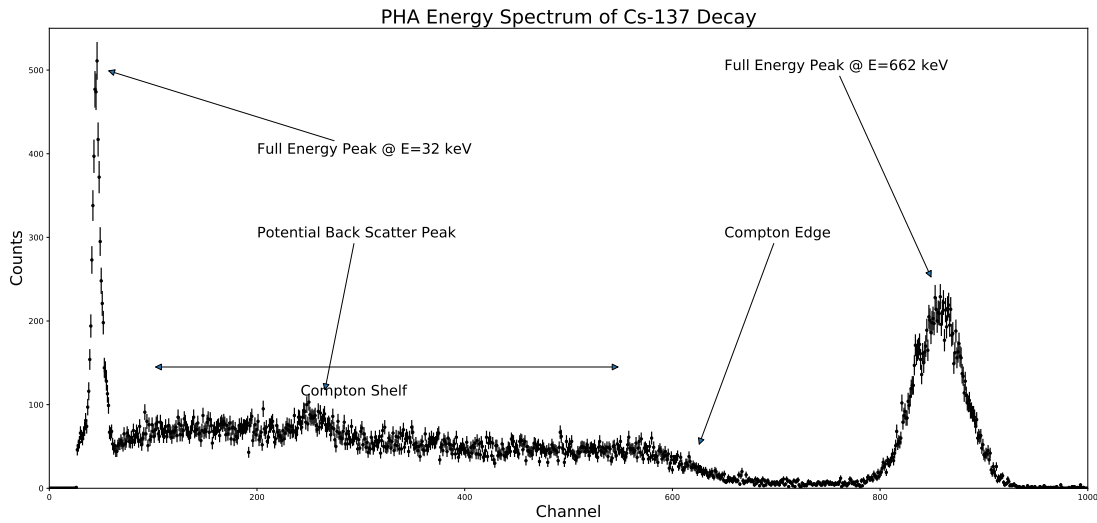


Figure 2: Full energy spectrum for Cs-137 Decay

percentages of probability of decaying with energy 276 keV, 382 keV, and 302 keV. These peaks affect the width of the 356 keV full energy peak expected. With other expected peaks that are nearby with lower possibility, it can bleed into the 356 keV full energy peak and make it much wider. This provides some uncertainty as to whether the counts measured by the software in this range really correspond to the 356 keV peak. This bleeding effect could account for the possible backscatter peak between 31 keV and 81 keV full energy peaks.

The region of interest is the range of channels around a peak that we identified as a full energy peak within the spectrum. To identify a region of interest, we would first look at a spectrum without any absorber to set our gains, and clearly identify any features that may arise. Our method of creating a

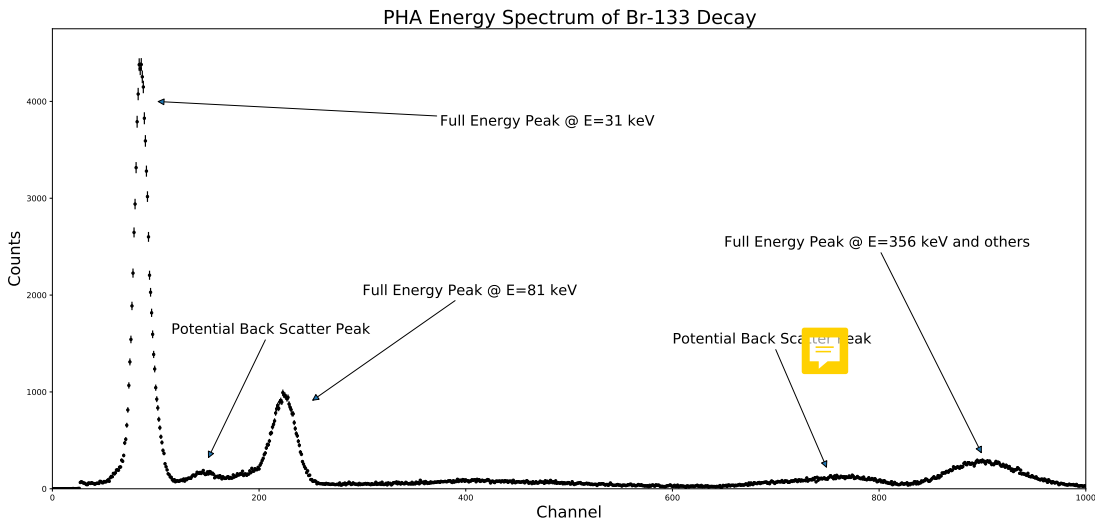


Figure 3: Full energy spectrum for Br-133 Decay

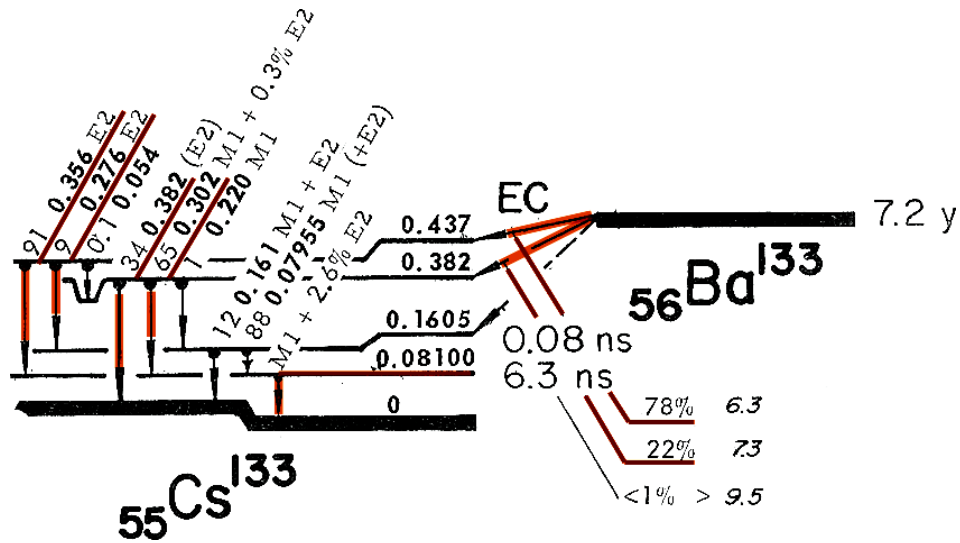


Figure 4: Nuclear Decay Scheme for Br-133

region of interest was to minimize the background counts that may come from peaks at higher energies. We would look at where the peak would level off on the left and right side. We would choose the side with the most counts, and match the height of that level to the other side. Our thinking behind this was that we would discount more background noise from potential bleeding from other energy peaks.

Using the software, we saved the histograms into tab separated values (*.tsv) files. With these tsv files and the numpy python library, we could easily identify and index into a region of interest to analyze a specific peak of our Sodium source near the expected 511 keV full energy peak.

Furthermore, we could provide a Gaussian fit to this clearly identified full energy peak, as can be seen in 5.

From this Gaussian fit, we can notice how high the background is as the fit predicts a constant

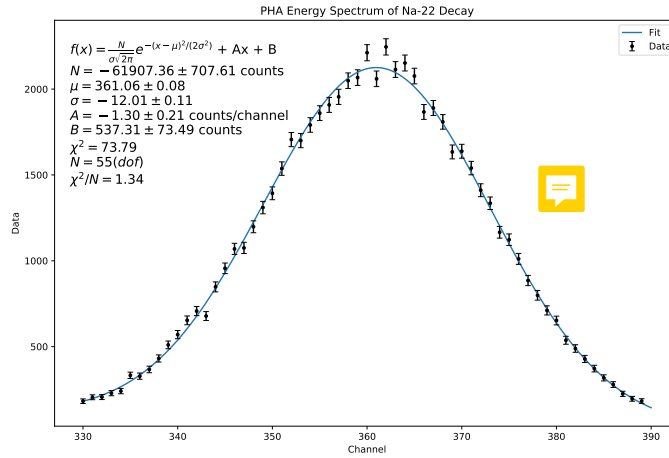


Figure 5: Gaussian fit to Na-22's 511 keV full energy peak

background term of 537.31 ± 73.49 counts. Despite being a rather well defined gaussian fit when comparing with other full energy peaks in the spectra by eye, this can point to the fact that there is a lot of background noise to be expected in further analysis.

2.2 Linear Attenuation Coefficient

Using the previously mentioned region of interest, we can make an exponential fit to the rate of change in the gross count per unit time as a function of the thickness of the absorber. This can serve as the fractional absorption mentioned earlier. Defining the rate of change in the counting per unit time as the gross count, this gets rid of any sort of background subtraction the software may have computed for the net count. Instead of the computer calculating a background amount within the region of interest, we will find that background count by fitting the rate of change in the gross count to a decaying exponential with an added constant term serving as the background. This would be the B constant in equation 3.

$$R(x) = R_0 e^{-\lambda x} + B \quad (3)$$

Using this idea, we can plot the count rate as a function of thickness, and extract a quantified linear attenuation coefficient, here noted as lambda.

From Figures 6, 7, and 8 that describe the transmission rate as a function of thickness, there are a couple abnormalities that arise that were not expected. In figure 7, the Cs-137 fit for the 662 keV full energy peak has very large uncertainties for the linear attenuation coefficient, and looks much more linear than exponential using the data. Also, the drop-off for a couple sources and peaks was much quicker than expected. The 31 keV peak for Ba-133 and 32 keV peak for Cs-137 shows the rates drop-off very quickly. However, since the linear attenuation coefficient should be correlated with the energy peak it is associated with, it makes sense for this similar characteristic to show within similar energy peaks. Even with steep drop offs, the fit still corresponds well with the data by eye.

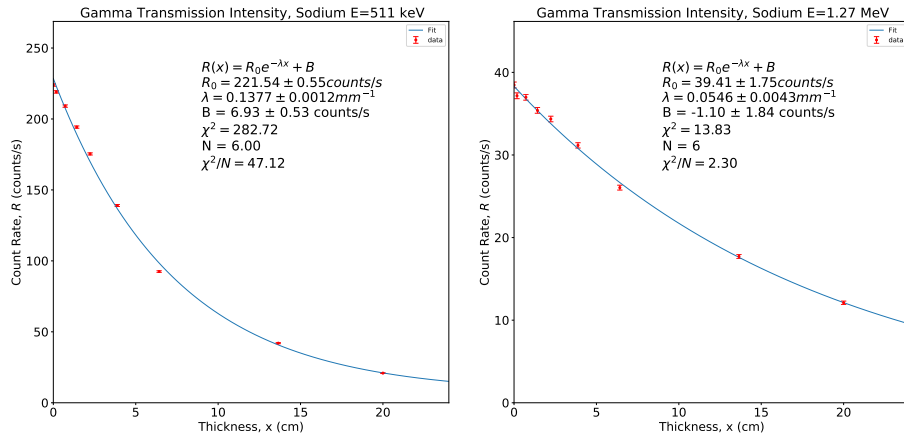


Figure 6: Exponential decay fit for Na-22 Decay

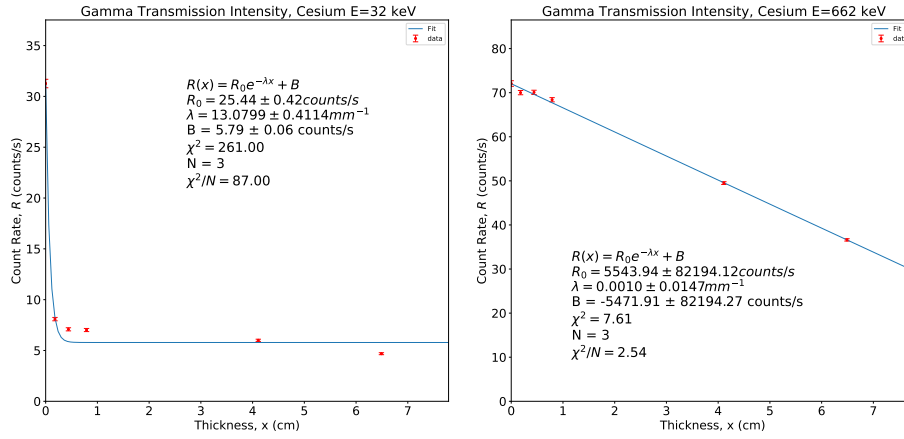


Figure 7: Exponential decay fit for Cs-137 Decay

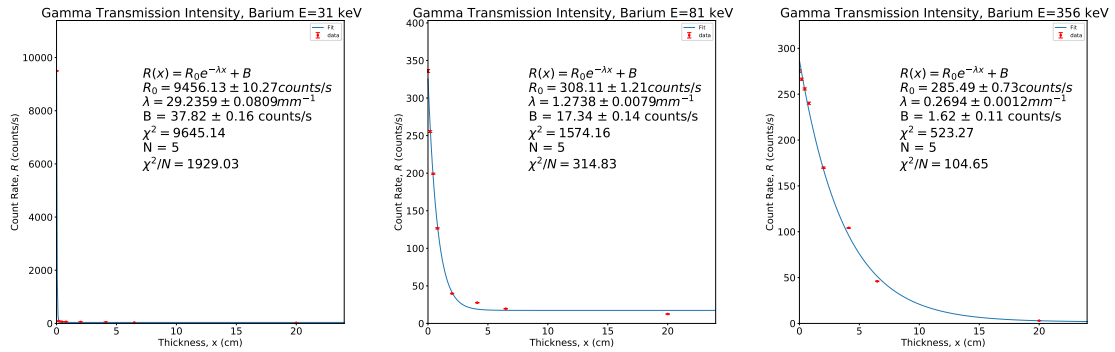


Figure 8: Exponential decay fit for Br-133 Decay

3 Discussion

3.1 Uncertainty

A couple different factors may affect the adequacy of our data. The uncertainty of the rate is first identified by the equation 4, where the rate is the $R = G/t$ and R is the average rate of change of the gross count.

$$\frac{dR}{R} = \sqrt{(\Delta G \frac{\partial R}{\partial G})^2 + (\Delta t \frac{\partial R}{\partial t})^2} = \sqrt{(\frac{\Delta G}{G})^2 + (\frac{\Delta t}{t})^2} \quad (4)$$


This uncertainty in the count rate is attributed to the uncertainty in the amount of counts, as well as the uncertainty in time. However, the uncertainty in time is very small. Here we approximate the uncertainty to 0.1s. This is because when we ran the experiment, we would set the software to stop after a set amount of time elapsed. The 0.1s is an estimation of the uncertainty in which the software communicates with the computer in order to both stop the counting, as well as to display the correct amount of counts. Leaving our experiment running for over 100 seconds, the overall contribution of time would be $0.1s/100s = 0.001$. For the large amount of time we would leave the experiment running for, the uncertainty for time is not as significant as the uncertainty in the count. Here, we assume $\Delta G = \sqrt{G}$, assuming Poisson statistics. The overall uncertainty in the count rate would be described as 5.

$$\frac{dR}{R} = \sqrt{(\frac{\Delta G}{G})^2} \quad (5)$$

Another source of uncertainty could be the region of interest chosen. Despite having explained our reasoning behind choosing the specific ROI we chose, it is still subjective and up to the user of the program to set some sort of region that will both encompass the full amount of the peak, while minimizing background. If our ROI is larger, the count rate would necessarily be larger since we are covering a larger energy spectrum to write down. Likewise, if the ROI is smaller, we get the specific region we would like, but we may miss a part of the peak. Either way, this would affect our uncertainty in the rate of the count, since it ends up simply being the square root of the gross count. A smaller ROI would increase the uncertainty, while a bigger ROI would minimize the significance of the counts within the peak.

After speaking with the lab professors, we learned that our method of minimizing the uncertainty in time, may affect the overall statistics of our findings. If we leave the software to count the gamma energy pulses passing through the absorber for the same amount of time for a run with no absorber and one with a thick absorber, the thick absorber will likely have a smaller count when the run finishes. This smaller amount of counts at a greater thickness will lead to greater uncertainty in the larger end of the figures. However, we didn't stick with this system. After finishing the runs for Sodium, we tried to vary the time we would set the software to stop the count. We would instead try to optimize setting the time so that our counts would be somewhere in the range of 10,000s of counts. A source of potential uncertainty that we managed was the physical setup of the experiment. Before starting to measure, we put the source relatively high from the table and closer to the crystal. This was to ensure we would receive a good amount of counts. Coming back Thursday to continue our experiment, we re-measured our setup to ensure it was the same that was left after running the experiment on Tuesday. Another source of potential uncertainty that was managed was the thickness of the lead absorbers for all of the runs. In theory, we could have measured just one of each of the three thicknesses of the absorbers provided. However, we re-measured the thickness for all different combinations of lead absorbers used using the micrometer, as some absorbers of the same type may be slightly different. Either way, the absorbers were measured with an uncertainty of ± 0.01 mm.

Lastly, the reduced chi-squared value for most of our plots are very high. From the seven exponential fits performed, only five have reduced chi-squared values that are less than 5. If the data were taken correctly and the uncertainty was properly accounted for, then the reduced chi-squared should be closer to 1. Despite having high values for this, simply looking at all of the plots show that the fits


do properly describe the trend of the data. Since it looks like the data follows the fit by eye, this goodness of fit parameter tells us that the error bars for the data are much too small to be purely from statistical randomness. Only a few of the data have error bars which lie within the fit. This shows that the data with fits having large reduced chi-squared values may have the uncertainty improperly accounted for. The uncertainty in the count rate may be much higher than expected, so there may be some systematic error that wasn't accounted for, such as any background sources from other groups that may have bled into  data. This sort of high background was previously noted when fitting a gaussian to Sodium's 511 full energy peak.

3.2 Comparison with Literature

Energy Peak (keV)	Measured λ (cm^{-1})	Literature λ (cm^{-1})	Cross Section σ (barns)
31	292.36 ± 0.81	311.46 ± 9.34	108.17525 ± 0.13044
32	130.08 ± 4.11	284.94 ± 8.55	48.39690 ± 0.05836
81	12.74 ± 0.08	26.00 ± 0.78	4.71312 ± 0.00568
356	2.69 ± 0.01	3.14 ± 0.09	0.99672 ± 0.00120
511	1.37 ± 0.01	1.79 ± 0.05	0.50935 ± 0.00061
662	0.01 ± 0.15	1.29 ± 0.04	0.00365 ± 0.00001
1270	0.55 ± 0.04	0.66 ± 0.02	0.20206 ± 0.00024

The literature linear attenuation coefficient is from NIST datasets which were interpolated using the python package `scipy`. Specifically, the method `interpolated.interp1d` with `kind = 'cubic'` was used to find values that are at the specific energy peaks of the sources used in the experiment. Also, the uncertainty of the cross section was calculated as $d\sigma = d\lambda/N$, where N is the number density for lead.

With the previously mentioned high reduced chi-squared values for many of the linear attenuation coefficients, the only results we can have some certainty about is the coefficient for Sodium's full energy peak around 1.27 MeV. The other low reduced chi-squared value for Cesium's 662 keV peak has large uncertainty for the linear attenuation coefficient when computing the fit for least-squares.

Comparing the linear attenuation coefficients that were computed to the literature, we can see that our data is mostly in agreement with the literature within an order of magnitude. However, there are no data in agreement within the error bars that were calculated using the least squares method. One anomaly that is apparent is the 662 keV linear attenuation coefficient. The value's error bars are too large in comparison to the fit to have much meaning. This is the fit that  looked very linear within the data taken shown in 7.

Since the measured linear attenuation coefficients are not clearly consistent with the literature, the cross sections cannot be reliably analyzed.

Theoretically, most of the linear attenuation coefficients should have a dominant absorption mechanism of the photoelectric effect. There starts being a discrepancy between the total absorption mechanism and the photoelectric effect around 200 keV, as can be seen in figure 9. So the dominant absorption mechanism for the 356 keV peak would still be photoelectric, but partly compton. Starting with Na-22's energy peak at 511 keV, the total effect is quite equal between the compton scattering and photoelectric effect. For Cs-137's full energy peak at 662 keV, compton scattering overtakes the photoelectric effect and is now the most dominant absorption mechanism. Lastly, Na-22's large 1.27 MeV energy peak also has compton scattering as the most dominant absorption mechanism.

Since all of our measured linear attenuation coefficients are underestimated when compared to the literature's value, the coefficients we have would lead to the conclusion that compton scattering is much more dominant than expected at an earlier energy level. However, since our reduced chi-squared is large and none of the measured linear attenuation coefficients with the error bars land inside of the literature's value, this characteristic cannot be concluded from the data measured. If we were confident in our results, a lower attenuation coefficient would correspond with a lower cross section of lead, or that the count rates drop off much slower than expected.

Pb

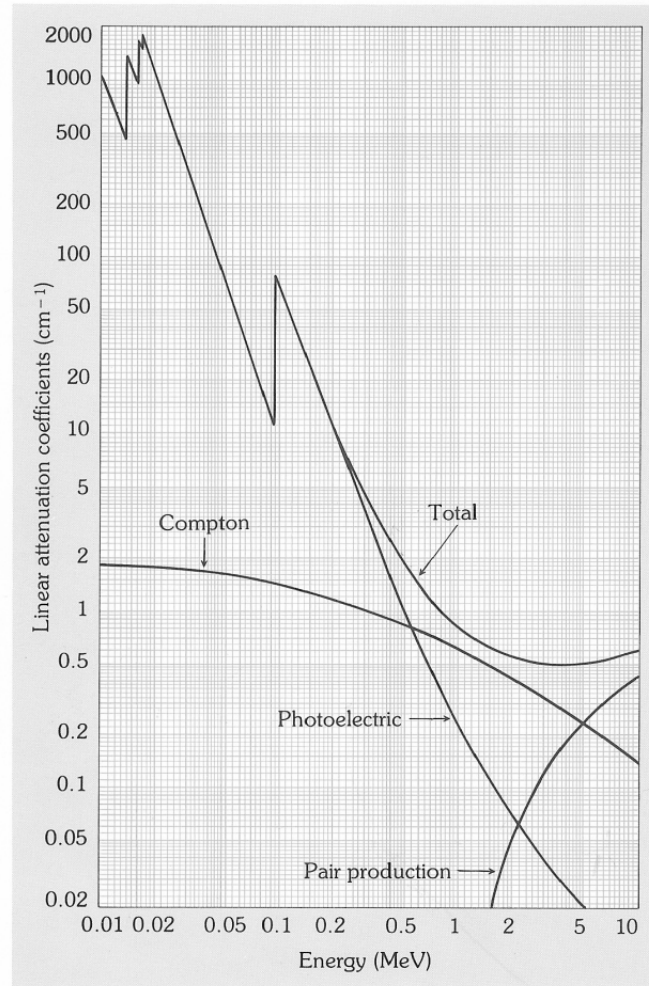


Figure 9: Linear Attenuation for Lead

Overall, there are few adequate conclusions that can be gathered from the data measured and uncertainties attributed with these data.

3.3 Future steps

Looking back on the overall experience of the experiment, there were a few areas where improvements could be made. When we chose to end the time is something that may have been thought through a bit more. Re-doing the experiment, I would try to optimize and aim for a couple tens of thousands of gross counts before ending the experiment. Either way, the effort that went into minimizing the time uncertainty was way too much, and could have been better spent.

Another potential avenue to make the data more adequate could be to optimize what actually makes the bins: change the gains. The runs completed had a set amount of coarse gain and fine gain that was optimized for when running the experiment with no absorber. Changing the gain may make a difference in how shallow or wide the gaussian peaks of the spectra are.

The 2 other ways to improve upon these results is to simply leave the detector running for a longer

period of time as well as using a greater number of absorber combinations. Many of our experiments were missing data for the thickness between the largest thickness used, $\frac{1}{2}$ half of that thickness. We focused on the thinner half of our thickness spectrum to ensure we had enough time to collect enough data for all 3 sources.

The final thing that could help align our measured data to the literature would be to complete a more rigorous analysis of the uncertainties that may have been attributed to the counts that the software measured.